Available online at www.sciencedirect.com
SCIENCE DIRECT®
Chemical Physics Letters 409 (2005) 208–211
CHEMICAL PHYSICS LETTERS
www.elsevier.com/locate/cplett

Band gap variation of size-controlled ZnO quantum dots synthesized by sol–gel method

Kuo-Feng Lin [a], Hsin-Ming Cheng [a,b], Hsu-Cheng Hsu [a], Li-Jiaun Lin [b], Wen-Feng Hsieh [a,*]

[a] *Department of Photonics and Institute of Electro-Optical Engineering, National Chiao Tung University, 1001 Tahsueh Road, Hsinchu 30050, Taiwan, Republic of China*
[b] *Material Research Laboratories, Industrial Technology Research Institute, Hsinchu 310, Taiwan, Republic of China*

Received 25 April 2005; in final form 7 May 2005
Available online 3 June 2005

Abstract

ZnO quantum dots were synthesized successfully via a simple sol–gel method. The average size of quantum dots can be tailored using well-controlled concentration of zinc precursor. Size-dependent blue shifts of photoluminescence and absorption spectra revealed the quantum confinement effect. The band gap enlargement is in agreement with the theoretical calculation based on the effective mass model. Furthermore, as the particle size decreases, we observed an increase in the size-dependent Stokes shift of the photoluminescence peak relative to the absorption onset.

1. Introduction

Semiconductor nanoparticles have recently attracted significant attention for their role in fundamental studies and technical applications [1,2], mainly due to their unusual photonic characteristics. Zinc oxide (ZnO) is a versatile material that has achievable applications in photo-catalysts, varistors, sensors, piezoelectric transducers, solar cells, transparent electrodes, electroluminescent devices and ultraviolet laser diodes. As a result, it has stimulated extensive research [3–13]. Compared to other wide band gap materials, ZnO has a large exciton binding energy of 60 meV, which results in efficient excitonic emission at room temperature. ZnO nanocrystals or quantum dots (QDs) have superior optical properties of the bulk crystals owing to quantum confinement effects. In the past decade, various methods have been employed to produce ZnO quantum QDs [14–21]. For instance, Guo et al. [15] experimentally established that the third-order nonlinear susceptibility of ZnO nanoparticles is almost 500 times larger than that of bulk ZnO. Vanmaekelbergh and co-workers [22] discovered that the optical transitions in artificial atoms consist of one to ten electrons occupying the conduction levels in ZnO nanocrystals. Fonoberov et al. [23] theoretically investigated that, depending on the fabrication technique and ZnO QD surface quality, the origin of UV photoluminescence (PL) in ZnO QDs is either recombination of confined excitons or surface-bound ionized acceptor–exciton complexes. More and more unique behaviors are continuously being explored.

Understanding the electronic and optical characterizations in ZnO QDs and nanoparticles is important from both a fundamental science and a proposed photonic application point of view. Accordingly, absorption spectra were widely used to investigate the band edge emission from ZnO QDs [14–20]. However, direct

* Corresponding author. Fax: +886 3 5716631.
E-mail address: wfhsieh@mail.nctu.edu.tw (W.-F. Hsieh).

0009-2614/$ - see front matter © 2005 Elsevier B.V. All rights reserved.
doi:10.1016/j.cplett.2005.05.027

observation of the band gap variation upon particle size from PL is relatively rare [21]. In this Letter, we show growth of high-quality ZnO QDs via a simple sol–gel method. The average size of nanoparticles can be tailored for use of the appropriate concentration of zinc precursor. Furthermore, size-dependent PL and absorption spectra are carefully discussed and compared with the theoretical calculation from the effective mass model.

2. Experimental

The ZnO colloidal solutions were produced from zinc acetate dihydrate (99.5% $Zn(OAc)_2$, Riedel-deHaen) in diethylene glycol (99.5% DEG, EDTA), similar to what we presented exhaustively before [24]. The slight difference is that we placed the final product in a centrifuge operating 3000 rpm for 30 min. After this procedure, the solution was separated into two gradations. The white bottom layer included the secondary ZnO clusters [24] and the upper suspension was more transparent and included the dispersive single crystalline ZnO QDs. Unlike the secondary clusters, the single crystalline ZnO QDs were almost monodispersive because of the stable surface during the chemical reaction. The average size of ZnO QDs can be tailored under well-controlled concentration of precursor, $Zn(OAc)_2$, including 0.04, 0.06, 0.08, 0.1, 0.16 and 0.32 M. The specimens were prepared by placing a drop of transparent suspension on glass substrates and carbon-coated copper grids were then allowed to air dry to remove excess solvent.

The shapes and sizes of ZnO QDs were analyzed using JEOL JEM-2100F field emission transmission electron microscope (FETEM) operated at 200 keV. The average crystallite sizes were also characterized using Bede D1 thin film X-ray diffractometer (TFXRD) with grazing incident mode. Optical absorption spectra were recorded on a Hitachi U4001 spectrophotometer with xenon lamp. The PL measurement was made using a 20 mW He–Cd laser at wavelength of 325 nm and the emission light was dispersed by a TRIAX-320 spectrometer and detected by a UV-sensitive photomultiplier tube.

3. Results and discussion

Fig. 1 shows a typical TEM micrograph of the ZnO QDs formed using 0.06 M $Zn(OAc)_2$. The nanoparticles are essentially little aggregated but still appear to be sphere and ellipsoid in shape individually. The mean-particle size is estimated to be $\sim 4.0 \pm 0.3$ nm. Presumably due to the viscosity of DEG, the solvent may have modified the Ostwald ripening kinetics such that the growth rate decreases with the size of the ZnO QDs. This would narrow the size distribution of ZnO QDs effectively.

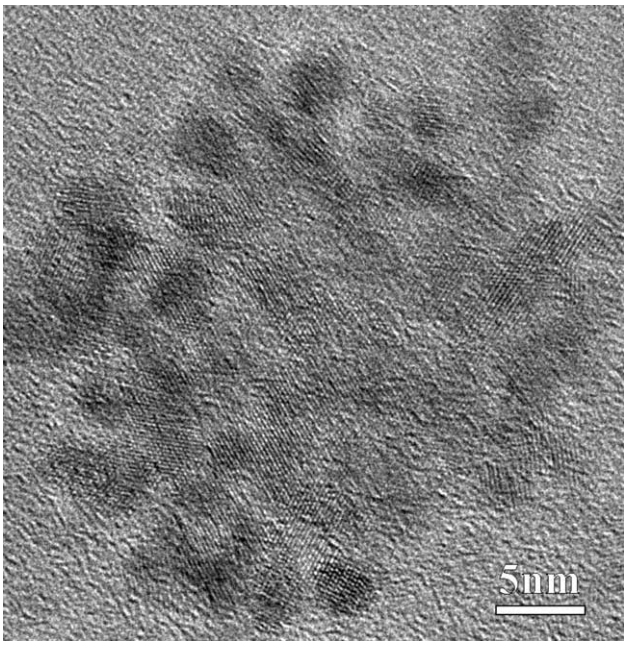

Fig. 1. TEM image of the ZnO QDs fabricated using 0.06 M $Zn(OAc)_2$.

Fig. 2 demonstrates the XRD profiles of the ZnO QDs prepared with various concentrations of $Zn(OAc)_2$. The diffraction peaks and their relative intensities of

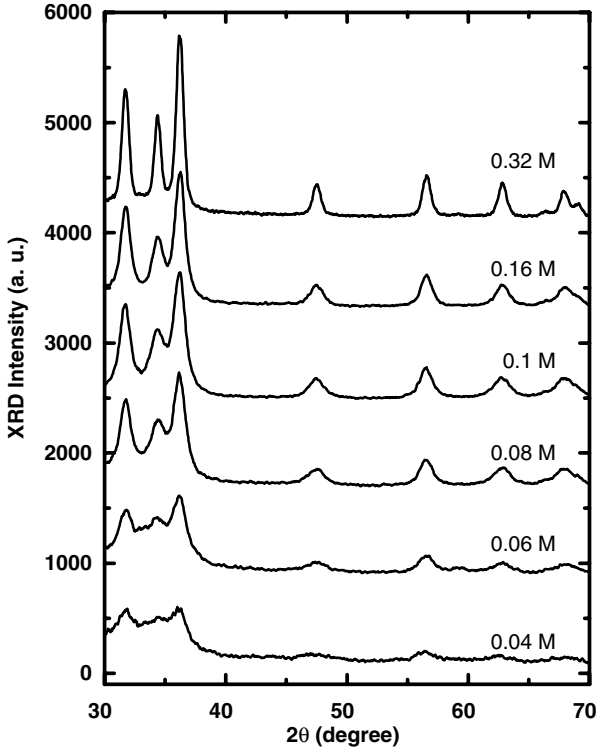

Fig. 2. XRD profiles of the ZnO QDs prepared with various concentration of $Zn(OAc)_2$. The crystalline size can be approximately estimated to be 12, 7.4, 6.5, 5.3, 4.2 and 3.5 nm, respectively (top to bottom), for concentration 0.32, 0.16, 0.1, 0.08, 0.06 and 0.04 M.

spectra all coincide with JCPDS card no. 36-1451, so that the observed patterns can be unambiguously attributed to the presence of hexagonal wurzite crystallites with cell constants of $a = 3.251$ Å and $c = 5.208$ Å. No excess peaks detected, which indicates that all the precursors have been completely decomposed and no other complex products were formed. It should be noted here that the full width at half maximum (FWHM) of the diffraction peaks increase while decreasing the concentration of zinc precursor duo to the size effect. Furthermore, the crystalline size can be estimated to be 12, 7.4, 6.5, 5.3, 4.2 and 3.5 nm, for concentration 0.32, 0.16, 0.1, 0.08, 0.06 and 0.04 M, respectively, by using the Debye–Scherer formula. The statistical result is consistent with the observation from TEM.

Fig. 3 shows typical PL and absorption spectra of samples with different average QD sizes. The UV emission represents a relaxed state of exciton near the band edge in ZnO QDs. The nature of the UV-PL from ZnO QDs itself is still a matter of controversy. Some authors attributed the UV-PL to the recombination of confined excitons [14], while others argued that the emission comes from surface impurities or defects [15]. In our case, high efficient UV emission near band edge is attributed to free exciton emission with high electronic density of states, which shift to higher energies from 3.30 to 3.43 eV as the QD size decreases from 12 to 3.5 nm. Since the exciton Bohr radius, a_B, of bulk ZnO is 2.34 nm [25], the Coulomb interaction should be relatively small as compared to the kinetic energy resulting from confinement in our samples and the ZnO QDs are in the moderate to strong confinement regime. In general, quantum confinement shifts the energy levels of the conduction and valence bands apart, giving rise to a blue shift in the transition energy as the particle size decreases. Such phenomenon is also revealed in the absorption spectra, although the faint excitonic absorption peaks due to the moderate size distribution of ZnO QDs. However, from this figure, it can clearly be seen that the absorption onset exhibits a progressive blue shift from 3.43 to 3.65 eV as the size of ZnO QD decreases. Similar observations of such size dependence upon optical properties have been made previously for other semiconductor quantum dots [26–28].

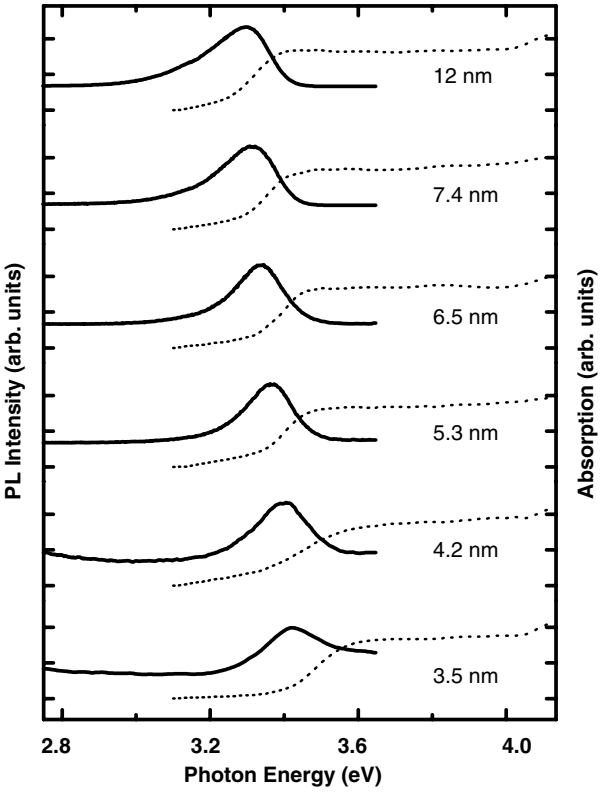

Fig. 3. PL (solid line) and absorption (dashed line) spectra near the band edge of various ZnO QD size.

The relationship between band gap and size of QD can be obtained using a number of models [29–32]. Using the effective mass model for spherical particles with a Coulomb interaction term [29], the band gap E_g^* [eV] can be approximately written as

$$E_g^* \cong E_g^{\text{bulk}} + \frac{\hbar^2\pi^2}{2er^2}\left(\frac{1}{m_e} + \frac{1}{m_h}\right) - \frac{1.8e^2}{4\pi\varepsilon\varepsilon_0 r}, \quad (1)$$

where E_g^{bulk} is the bulk energy gap, r is the particle radius, m_e is the effective mass of the electrons, m_h is the effective mass of the holes, ε is the relative permittivity, ε_0 is the permittivity of free space, $\hbar$ is Planck's constant divided by 2π , and e is the charge of the electron. The polarization term included in this model is usually negligible.

Fig. 4 shows both the UV emission peaks, absorption onsets and the dependence of the band gap enlargement

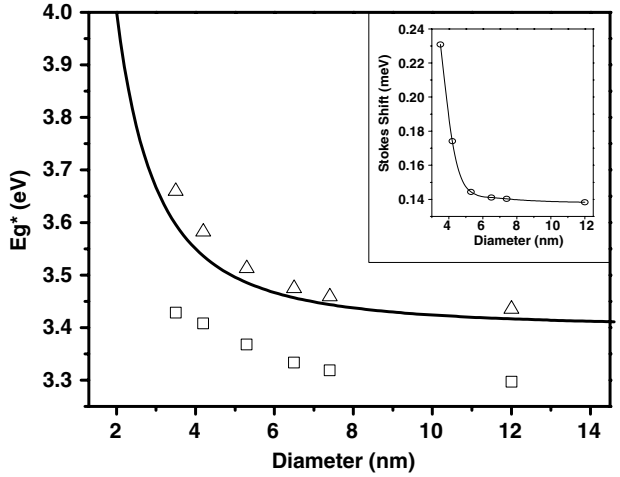

Fig. 4. The dependence of the band gap enlargement versus the ZnO QDs diameter as calculated from the effective mass model and the corresponding experimental data of PL peak maximum (□) and the absorption onset (△). The inset shows the size-dependent Stokes shift of various QD diameter.

on the ZnO QD diameter as calculated from the effective mass model (Eq. (1)) with $E_g^{bulk} = 3.35$ eV, $m_e = 0.24m_0$, $m_h = 0.45m_0$, and $\varepsilon = 3.7$, where m_0 is the free electron mass [33]. Enlargement effects are expected to be predominant when the QD size is less than 6 nm, meanwhile PL data and absorption data of the same tendency indicates effective mass theories accurately, which predict the size-dependent energy gap. We note here that the absorption data closely coincides with the curve calculated from the effective mass model. However, the PL data is not fixed since it represents the emission from a relaxed state and the exciton binding energy should be considered. We also observed a size-dependent Stokes shift of the PL maximum relative to the absorption onset as shown in the inset of Fig. 4. This Stokes shift increases as the particle size decreases and has been observed in other II–VI and III–V QDs (e.g., InP, CdSe) and extrapolated exponentially or hyperbolically [34]. Such a presentation was previously reported as either size-dependent electron–phonon processes or size-dependent spin–orbit exchange interaction, which may contribute to the Stokes shift. However, the origin of the size-dependent Stokes shift in semiconductor QD systems remains unclear at present [34,35].

4. Conclusion

In summary, we have demonstrated successfully the ZnO QDs synthesized by a simple sol–gel method and the average size of ZnO QDs can be tailored under well-controlled concentration of zinc precursor. Size-dependence of efficient UV photoluminescence and absorption spectra of various QD sizes give evidence for the quantum confinement effect. Furthermore, band gap enlargement is also in agreement with the theoretical calculation based on the effective mass model. We also observed an increase in size-dependent Stokes shift of the PL maximum relative to the absorption onset as the particle size decreases.

Acknowledgements

Authors gratefully acknowledge financial support from the National Science Council (NSC) in Taiwan under Contract No. NSC-93-2112-M-009-035. We also thank the Nano Technology Research Center and Energy & Resources Laboratories of ITRI for facilitates support and S.Y. Lai (TEM group of MRL/ITRI) for great help on electron microscopy measurements.

References

[1] J.R. Heath, Ed. Acc. Chem. Res. 32 (1999) 389 (Special issue for Nanoscale Materials).
[2] A.P. Alivisatos, Science 271 (1996) 933.
[3] F.C. Lin, Y. Takao, Y. Shimizu, M. Egashira, Sensors Actuators B 24–25 (1995) 843.
[4] K.S. Weissenrieder, J. Muller, Thin Solid Films 30 (1997) 300.
[5] J. Muller, S. Weissenrieder, J. Anal. Chem. 349 (1994) 380.
[6] S.C. Minne, S.R. Manalis, C.F. Quate, Appl. Phys. Lett. 67 (1995) 3918.
[7] Karin. Keis, Nanostructured ZnO Electrodes for Solar Cell Applications, Acta Universitatis Upsaliensis, Uppsala, 2001.
[8] J.B. Baxter, E.S. Aydil, Appl. Phys. Lett. 86 (2005) 053114.
[9] R.L. Hoffman, B.J. Norris, J.F. Wager, Appl. Phys. Lett. 82 (2003) 733.
[10] W.I. Park, G.C. Yi, Adv. Mater. 16 (2003) 1907.
[11] R. Könenkamp, R.C. Word, C. Schlegel, Appl. Phys. Lett. 85 (2004) 6004.
[12] Z.K. Tang, G.K.L. Wong, P. Yu, M. Kawasaki, A. Ohtomo, H. Koinuma, Y. Segawa, Appl. Phys. Lett. 72 (1998) 3270.
[13] T. Makino, C. Chia, Y. Segawa, M. Kawasaki, A. Ohtomo, K. Tamura, Y. Matsumoto, H. Koinuma, Appl. Surf. Sci. 189 (2002) 277.
[14] D.W. Bahnemann, C. Kormann, M.R. Hoffmann, J. Phys. Chem. 91 (1987) 3789.
[15] L. Guo, S. Yang, C. Yang, P. Yu, J. Wang, W. Ge, G.K.L. Wong, Appl. Phys. Lett. 76 (2000) 2901.
[16] E.A. Meulenkamp, J. Phys. Chem. B 102 (1998) 5566.
[17] E.M. Wong, J.E. Bonevich, P.C. Searson, J. Phys. Chem. B 102 (1998) 7770.
[18] S. Sakohara, M. Ishida, M.A. Anderson, J. Phys. Chem. B 102 (1998) 10169.
[19] S. Mahamuni, K. Borgohain, B.S. Bendre, V.J. Leppert, S.H. Risbud, J. Appl. Phys. 85 (1999) 2861.
[20] H. Zhou, H. Alves, D.M. Hofmann, W. Kriegseis, B.K. Meyer, G. Kaczmarczyk, A. Hoffmann, Appl. Phys. Lett. 80 (2002) 210.
[21] E.M. Wong, P.C. Searson, Appl. Phys. Lett. 74 (1999) 2939.
[22] A. Germeau, A.L. Roest, D. Vanmaekelbergh, G. Allan, C. Delerue, E.A. Meulenkamp, Phys. Rev. Lett. 90 (2003) 097401.
[23] V.A. Fonoberov, A.A. Balandin, Appl. Phys. Lett. 85 (2004) 5971.
[24] H.M. Cheng, H.C. Hsu, S.L. Chen, W.T. Wu, C.C. Kao, L.J. Lin, W.F. Hsieh, J. Cryst. Growth 277 (2005) 192.
[25] R.T. Senger, K.K. Bajaj, Phys. Rev. B 68 (2003) 045313.
[26] D.J. Norris, Al.L. Efros, M. Rosen, M.G. Bawendi, Phys. Rev. B 53 (1996) 16338.
[27] C.A. Smith, H.W.H. Lee, V.J. Leppert, S.H. Risbud, Appl. Phys. Lett. 75 (1999) 1688.
[28] H. Zhang, L.P. Wang, H.M. Xiong, L.H. Hu, B. Yang, W. Li, Adv. Mater. 15 (2003) 1712.
[29] L.E. Brus, J. Chem. Phys. 80 (1984) 4403.
[30] M.S. Hyberstsen, Phys. Rev. Lett. 72 (1994) 1514.
[31] A.L. Efros, M. Rosen, Annu. Rev. Mater. Res. 30 (2000) 475.
[32] K.E. Andersen, C.Y. Fong, W.E. Pickett, J. Non Cryst. Solids 299 (2002) 1105.
[33] S.A. Studenikin, N. Golego, M. Cocivera, J. Appl. Phys. 84 (1998) 2287.
[34] H. Fu, A. Zunger, Phys. Rev. B 56 (1997) 1496.
[35] M. Nirmal, D.J. Norris, M. Kuno, M.G. Bawendi, Al.L. Efros, M. Rosen, Phys. Rev. Lett. 75 (1995) 3728.